Astronomy & Astrophysics

VLT/X-shooter Spectroscopy of a dusty planetary nebula discovered with *Spitzer*/IRS
(Research Note)

I. Oliveira[1], R. A. Overzier[2], K. M. Pontoppidan[3], E. F. van Dishoeck[1,4], and L. Spezzi[5]

[1] Leiden Observatory, Leiden University, PO Box 9513, 2300 RA Leiden, The Netherlands
    e-mail: oliveira@strw.leidenuniv.nl
[2] Max-Planck-Institut für Astrophysik, Karl-Schwarschild-Str. 1, 85741 Garching, Germany
[3] California Institute of Technology, Division for Geological and Planetary Sciences, MS 150-21, Pasadena, CA 91125, USA
[4] Max-Planck Institut für Extraterrestrische Physik, Giessenbachstrasse 1, 85748 Garching, Germany
[5] Research and Scientific Support Department, European Space Agency (ESA-ESTEC), PO Box 299, 2200 AG Noordwijk,
    The Netherlands

ABSTRACT

As part of a mid-infrared spectroscopic survey of young stars with the *Spitzer* Space Telescope, an unclassified red emission line object was discovered. Based on its high ionization state indicated by the *Spitzer* spectrum, this object could either be a dusty supernova remnant (SNR) or a planetary nebula (PN). In this research note, the object is classified and the available spectroscopic data are presented to the community for further analysis. UV/optical/NIR spectra were obtained during the science verification run of the VLT/X-shooter. A large number of emission lines are identified allowing the determination of the nature of this object. The presence of strong, narrow ($\Delta v \sim 8 - 74$ km s^{-1}) emission lines, combined with very low line ratios of, e.g., [N II]/Hα and [S II]/Hα show that the object is a PN that lies at an undetermined distance behind the Serpens Molecular Cloud. This illustrates the potential of X-shooter as an efficient tool for constraining the nature of faint sources with unknown spectral properties or colors.

Key words. planetary nebulae: general – line: identification

1. Introduction

As part of a program with the InfraRed Spectrograph (IRS, Houck et al. 2004) onboard the *Spitzer* Space Telescope (SST, Werner et al. 2004) aimed at characterizing the circumstellar disks of a flux-limited sample of infrared-excess young stellar objects (YSOs) in the Serpens Molecular Cloud ($\alpha_{J2000} = 18^h29^m49^s$, $\delta_{J2000} = +01^d14^m48^s$), an interesting object of unknown nature was discovered (SSTc2dJ18282720+0044450, or #17 in Oliveira et al. 2010, hereafter OL17). The very bright, high ionization emission lines seen in the mid-IR spectrum of this object are not consistent with it being a YSO.

Two types of galactic objects show such high excitation lines: dusty planetary nebulae (PNe, Bernard-Salas et al. 2009; Stanghellini et al. 2007; Guiles et al. 2007) and supernova remnants (SNRs, Sandstrom et al. 2009; Ghavamian et al. 2009). SNRs typically show very broad emission lines, produced by the high velocity shock waves (Fesen et al. 1985; Fesen & Hurford 1996; Stupar et al. 2007). PNe, on the other hand, are characterized by narrow emission lines arising from the low velocity expanding outer shells (Balick & Frank 2002; Górny et al. 2009). Both classes of objects have been extensively studied by several authors, although just a few are so dusty that they were initially discovered only at mid-infrared wavelengths. To distinguish between these two possibilities, further spectroscopy on OL17 was needed.

In this research note, we present the original IRS spectrum (Sect. 2) as well as follow-up VLT/X-shooter spectra obtained as part of the instrument science verification phase (Sect. 3) and report on our identification of this object as a PN (Sect. 4).

2. *Spitzer*/IRS data

The IRS spectrum of OL17 ($\alpha_{J2000} = 18^h28^m27.2^s$, $\delta_{J2000} = +00^d44^m45^s$) is presented in Fig. 1. The data were obtained as part of the SST Cycle 3 program (GO3 30223, PI: Pontoppidan) in the low-resolution module ($R = \lambda/\Delta\lambda = 50$–100; short low [SL], 5.2–14.5 μm and long low [LL], 14.0–38.0 μm). See Oliveira et al. (2010) for further details on the program and the procedures for data reduction.

The spectrum is dominated by strong [O IV] emission[1] at 25.89 μm, and is accompanied by other prominent high ionization lines: [Ar III] (8.99 μm), [S IV] (10.51 μm), [Ar V] (13.07 μm), [Ne V] (14.32, 24.32 μm), [Ne III] (15.56 μm), and [S III] (18.71 μm, 33.48 μm). The equivalent width (*EW*) of these lines, calculated from Gaussian fits, as well as the line fluxes are given in Table 1. Furthermore, the spectrum shows clear evidence for polycyclic aromatic hydrocarbon (PAH) emission (most notably at 6.2, 7.7, 11.2, and 12.8 μm). This emission most likely comes from a shell of dusty material that surrounds, and is illuminated by, the central object.

---

[1] In principle, the [O IV] may suffer from contamination by [Fe II] at the resolution of the LL module, but this is ruled out in this case following our conclusion that this object is a PN and given that [Fe II] is relatively weak in such objects.
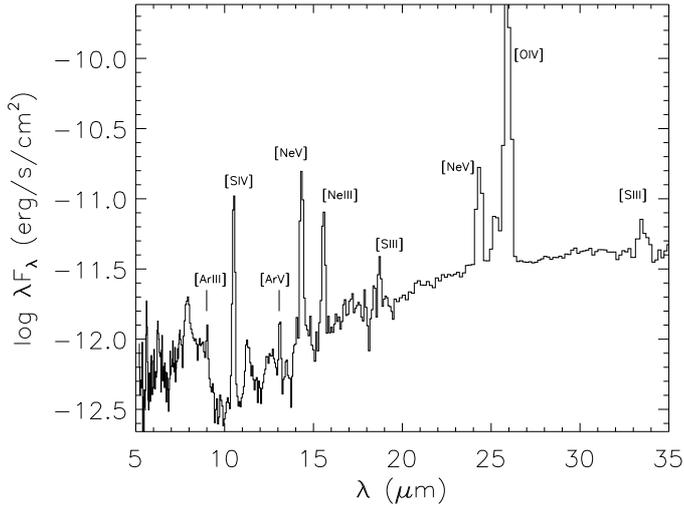
Fig. 1. IRS spectrum of OL17, a PN/SNR candidate found among the sample from Oliveira et al. (2010). The [O IV] line (25.89 μm) clearly dominates the spectrum.

Table 1. Emission lines identified in the IRS spectrum of OL17 (Fig. 1).

λ (μm)	Line	EW (μm)	Flux (erg/s/cm^2)
8.99	[Ar III]	0.08	6.15×10^{-15}
10.51	[S IV]	2.91	1.26×10^{-13}
13.07	[Ar V]	0.14	6.89×10^{-15}
14.32	[Ne V]	3.23	1.88×10^{-13}
15.56	[Ne III]	1.11	8.30×10^{-14}
18.71	[S III]	0.23	2.03×10^{-14}
24.32	[Ne V]	1.45	1.92×10^{-13}
25.89	[O IV]	13.64	2.81×10^{-12}
33.48	[S III]	0.31	3.80×10^{-14}

Because OL17 lies along the line of sight towards the Serpens Molecular Cloud, it is appreciably extincted due to foreground material ($A_V \sim 6.0$ mag). It has weak detections in both the R-band and IRAC1 band (3.5 μm), but is very prominent in the MIPS1 band (24 μm). It has a 3–24 μm slope ($\frac{d \log(\lambda F_\lambda)}{d \log(\lambda)}$) of ≈ 1.8. As shown in Fig. 1, the MIPS1 band is dominated by the very strong [O IV] emission line. This explains why this object appeared so red in the infrared color-magnitude diagrams, leading to the original misclassification of the source as an YSO. The optical R-band image taken with the Wide Field Camera (WFC) on the Isaac Newton Telescope (INT, Spezzi et al. 2010), the IRAC1 (Harvey et al. 2006) and MIPS1 (Harvey et al. 2007) images are shown in Fig. 2 (see Table 2 for the photometry in different bands).

3. X-shooter data

X-shooter (D'Odorico et al. 2006) is a unique multi-wavelength (300–2480 nm) medium resolution ($R = 4000-14\,000$) spectrograph on the Cassegrain focus of UT2 on the Very Large Telescope (VLT). It consists of 3 independent arms that give simultaneous spectra long-ward of the atmospheric cutoff in the UV ("UVB" arm), optical ("VIS" arm) and near-infrared ("NIR" arm). The data[2] presented here were obtained as part of the X-shooter 2nd science verification phase (SV2), during September–October 2009, PI: Oliveira). The total amount
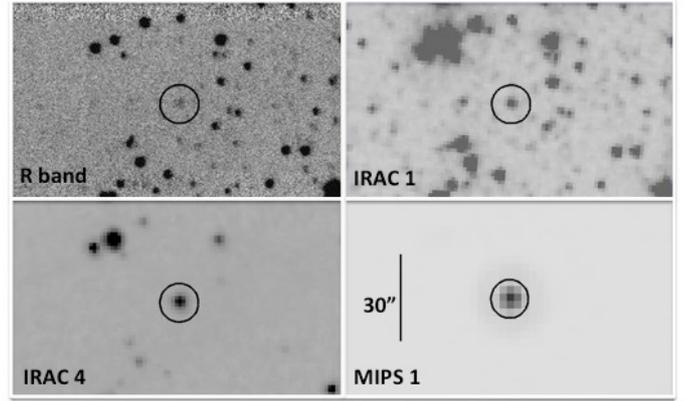
_____

[2] Program ID 60.A-9416(A).

Fig. 2. Optical and infrared images showing the INT/WFC R-band (*top-left*), IRAC1 (*top-right*), IRAC4 (*bottom-left*) and MIPS1 (*bottom-right*). All three images display the same field of view and a length scale of 30″ is shown for reference.

Table 2. Optical R-band magnitude and *Spitzer* IRAC/MIPS fluxes of OL17 (see also Fig. 2).

$R^\dagger$ (mag)	3.6 μm (mJy)	4.5 μm (mJy)	5.8 μm (mJy)	8.0 μm (mJy)	24.0 μm (mJy)
22.8	0.28	0.64	0.80	2.29	69.60

Notes. [†] From Spezzi et al. (2010).

of time awarded was 1 hr, during which integrations of 2760, 2560 and 2880s were obtained with the UVB, VIS and NIR arms, respectively. The observations were performed using the $1'' \times 12''$ slit in "nodding-on-slit" mode to perform adequate background subtraction in the near-infrared. The spectral resolving powers achieved in this setup were ≈5100 in UVB and NIR and ≈8800 in VIS. The raw science data consist of images containing highly curved, multi-order, two-dimensional spectra that need to be rectified, wavelength calibrated and merged using an input model configuration that describes the X-shooter spectral format. Data reduction was performed using an internal release of the X-shooter data calibration pipeline version 0.9.4 (Andrea Modigliani, priv. comm.), together with the "com4" reference calibration data.

The extracted one-dimensional spectra are shown in Fig. 3, and show many strong, narrow emission lines especially in the optical and NIR. These spectra were extracted using an aperture with a length of ~5″ in order to include most of the extended emission seen along the slit (see top panel of Fig. 4 for the two-dimensional spectrum). Since OL17 is seen through a dense molecular cloud, it is very faint. These exposures therefore allowed the detection of the brightest emission lines, but not the continuum. Although the spectra were not flux calibrated, the analysis below makes use of line ratios involving lines that are closely spaced in wavelength, and not affected by strong telluric absorption bands.

The main lines identified, and their EWs are listed in Table 3. The EWs were calculated by fitting the lines and a possible continuum using a Gaussian profile and should be considered (3σ) lower limits, as the continuum was not detected at a sufficient signal-to-noise in these observations. It is interesting to note that the faintness of the continuum as inferred from the optical spectrum implies that the object detected in the R-band image shown in the top-left panel of Fig. 2 must consist almost entirely of Hα line emission.
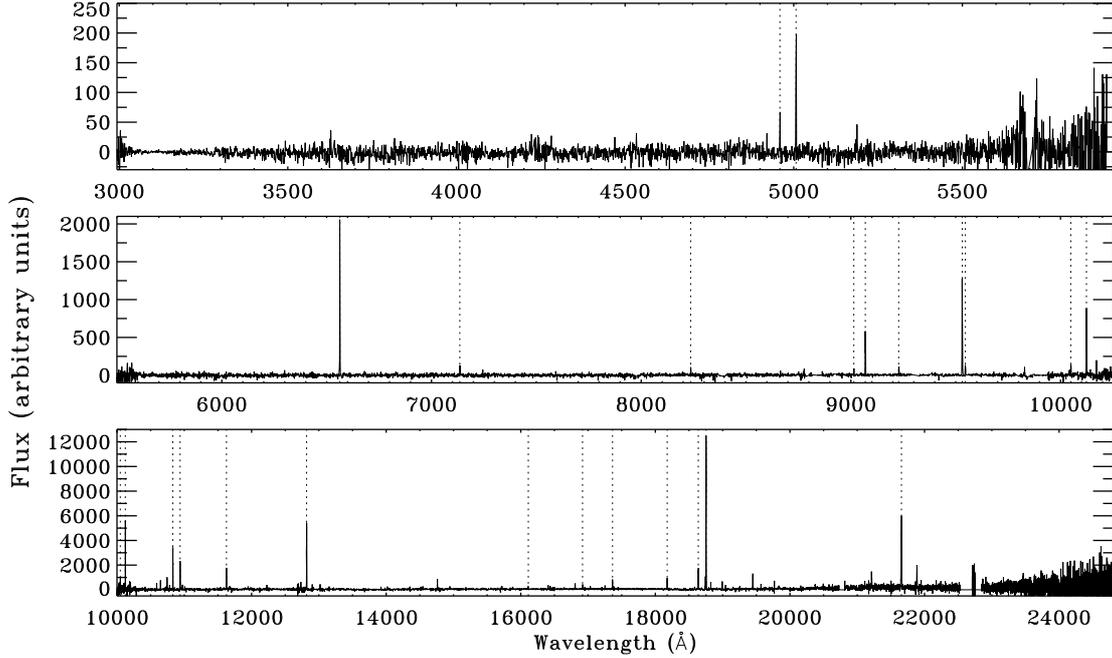
Fig. 3. X-shooter spectra of OL17. Panels show the one-dimensional spectra extracted from the UV/blue (*top*), the visible (*middle*), and the near-infrared (*bottom*) arms. Dotted lines mark the major emission lines tabulated in Table 3.
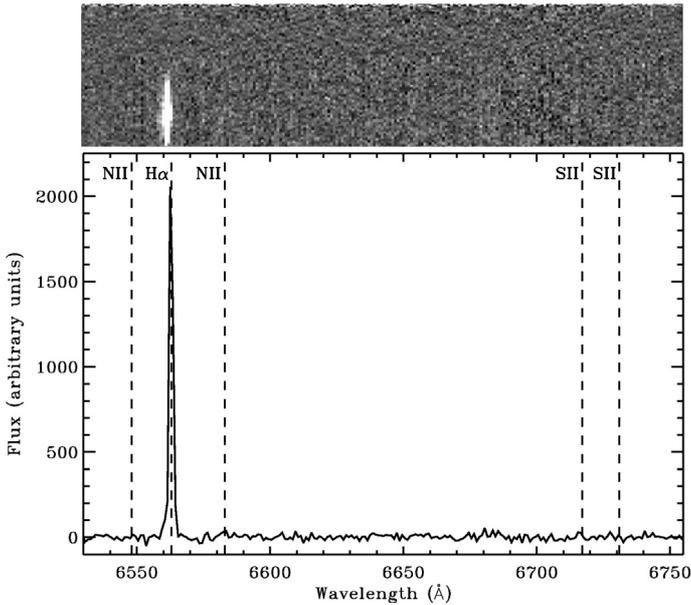

Fig. 4. A zoom-in of the optical spectrum covering Hα and the [N II] and [S II] line doublets. The weakness of [N II] and [S II] relative to Hα indicate that this object is a PN and not a SNR (see Sect. 4 for details). The top panel shows the two-dimensional spectrum at corresponding wavelengths (white pixels indicate large, positive pixel values). The slit height measures 12″, while the spatial extent of the resolved Hα is about 6″.

4. Results

According to Fesen et al. (1985), the main quantitative criterion used to distinguish SNRs from PNe is the strength of the [S II] ($\lambda\lambda6717, 6731$ Å) emission lines relative to that of Hα. That is, [S II]/Hα > 0.4 for typical SNRs (Matonick & Fesen 1997; Blair & Long 2004). Furthermore, SNRs typically have very strong [N II] ($\lambda\lambda6548, 6583$ Å) emission. Figure 4 shows a zoom of the X-shooter/VIS spectrum in the wavelength range covering

Table 3. Major emission lines identified in the X-shooter spectra (Fig. 3).

λ (Å)	Line	EW (Å)	λ (Å)	Line	EW (Å)
4959	[O III]	1.4	10831	He I	196.1
5007	[O III]	5.1	10938	H I	125.7
6563	Hα	47.1	11627	He II	100.4
7135	[Ar III]	2.6	12818	H I	290.5
8236	He II	2.9	16112	O I	21.9
9014	H I	2.4	16918	Al II	25.6
9069	[S III]	18.8	17364	Ne II	66.0
9229	H I	5.5	18176	Ne II	88.1
9531	[S III]	43.4	18638	Ne II	183.4
9546	H I	22.2	18754	N II	564.4
10049	H I	5.4	21657	Br γ	597.1
10123	He II	228.5			

Notes. Equivalent widths (*EW*) given indicate (3σ) lower limits, due to the faintness of the continuum.

Hα and the [N II] and [S II] doublets as labelled. It is clearly seen that the [N II] and [S II] lines are not detected, while Hα is very strong. Upper limits for the undetected lines were derived, yielding a flux ratio of [N II]/Hα ∼ [S II]/Hα ≤ 0.06 (3σ). This value is well below the value of 0.4 quoted above as the lower threshold for SNRs.

Furthermore, SNRs have broad, high velocity ($\Delta v \geq 300$ km s^{-1}) emission lines, while PNe show much narrower lines. This criterion was used by Fesen & Milisavljevic (2010) to classify the *Spitzer* source J222557+601148, previously believed to be a young galactic SNR (Morris et al. 2006), as a PN. As it can be seen in Fig. 5 for a selection of lines in all 3 X-shooter arms, the typical *FWHM* for lines seen in these data are <15–74 km s^{-1} (deconvolved for instrumental resolutions of *FWHM* ∼ 59 in UVB/NIR and 34 km s^{-1} in VIS). The low velocity of the lines, combined with the low ratio of [S II]/Hα ≤ 0.06 allow the conclusion that OL17 is a PN and not a SNR.
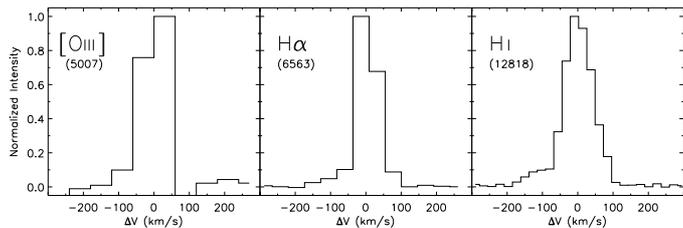
Fig. 5. A sample of the narrow emission lines present in the X-shooter spectra: [O III] (*left*) at 5007 Å, Hα (*middle*) and H I (Paβ, *right*) at 12 818 Å.

The electron density (n_e) can be derived from the ratio between the [S III] lines at 33.48 and 18.71 μm in the IRS spectrum, using the method of Herter et al. (1982). The ratio of [S III]λ33.48/18.71 $\sim$ 1.9 yields an electron density of $\sim$1–100 cm^{-3} (Rubin 1989), where the large range is due to the fact that we are in the regime where the line ratio is least sensitive to the density. However, we should note that the line at 33.47 μm appears to be twice as broad as that at 18.71 μm (possibly due to a data artifact). If we conservatively estimate that $\sim$50% of the flux in this line is indeed due to contamination, the [S III] 33.47/18.71 ratio would yield a density of order 1000 cm^{-3}, more typical of PNe. In any case, we note that unlike the intensity ratios of [N II]/Ha and [S II]/Hα, n_e is a rather poor diagnostic for discriminating between SNRs and PNe as both span a similarly large range in density (Sabbadin et al. 1977; Riesgo & López 2005).

While the distance to this PN cannot be determined without knowing its intrinsic size, its angular extent of $\approx$6$''$ (determined from the extent of Hα in the two-dimensional spectrum) and the large extinction it experiences in the bluer parts of the spectrum suggest that this PN must lie at a distance of at least several kpc, i.e., firmly behind the Serpens Molecular Cloud (distance of $\sim$415 pc, Dzib et al. 2010).

We summarize as follows:

1. The *Spitzer*/IRS spectrum of SSTc2dJ18282720+0044450 from Oliveira et al. (2010) shows strong high ionization emission lines, compatible with both Planetary Nebulae and Supernova Remnants, one of only a handful such objects identified in the mid-IR to date.
2. High quality VLT/X-shooter spectra, obtained during the science verification run, show a wealth of narrow emission lines in the UV/blue, optical and near-IR arm data, illustrating the enormous potential of X-shooter as a diagnostic tool for optically faint sources discovered at other wavelengths.

3. The optical line ratios are compatible with PNe and not with SNRs: the low values measured for the line ratio [S II]/Hα, one of the main diagnostic criteria for distinguishing between the two types of objects, allows a straightforward classification of this object as a PN.
4. The PN interpretation is confirmed by the relative narrow ($\Delta v \sim$ 8–74 km s^{-1}) width of the emission lines seen throughout the spectra.
5. This previously unknown PN now has public, high-quality spectroscopic data covering a very large bandwidth ranging from 0.3 to 35 μm. We encourage the use of these data[3] by the community wishing to further study objects of this class.

References

Balick, B., & Frank, A. 2002, ARA&A, 40, 439
Bernard-Salas, J., Peeters, E., Sloan, G. C., et al. 2009, ApJ, 699, 1541
Blair, W. P., & Long, K. S. 2004, ApJS, 155, 101
D'Odorico, S., Dekker, H., Mazzoleni, R., et al. 2006, Proc. SPIE, 6269, 98
Dzib, S., Loinard, L., Mioduszewski, A. J., Boden, A. F., Rodríguez, L. F., & Torres, R. M. 2010, ApJ, 718, 610
Fesen, R. A., & Hurford, A. P. 1996, ApJS, 106, 563
Fesen, R. A., & Milisavljevic, D. 2010, AJ, 139, 2595
Fesen, R. A., Blair, W. P., & Kirshner, R. P. 1985, ApJ, 292, 29
Ghavamian, P., Raymond, J. C., Blair, W. P., et al. 2009, ApJ, 696, 1307
Górny, S. K., Chiappini, C., Stasińska, G., & Cuisinier, F. 2009, A&A, 500, 1089
Guiles, S., Bernard-Salas, J., Pottasch, S. R., & Roellig, T. L. 2007, ApJ, 660, 1282
Harvey, P. M., Chapman, N., Lai, S.-P., et al. 2006, ApJ, 644, 307
Harvey, P. M., Rebull, L. M., Brooke, T., et al. 2007, ApJ, 663, 1139
Herter, T., Briotta, D. A., Jr., Gull, G. E., Shure, M. A., & Houck, J. R. 1982, ApJ, 262, 164
Houck, J. R., Roellig, T. L., van Cleve, J., et al. 2004, ApJS, 154, 18
Matonick, D. M., & Fesen, R. A. 1997, ApJS, 112, 49
Morris, P. W., Stolovy, S., Wachter, S., et al. 2006, ApJ, 640, L179
Oliveira, I., Pontoppidan, K. M., Merín, B., et al. 2010, ApJ, 714, 778
Riesgo, H., & López, J. A. 2005, Rev. Mex. Astron. Astrofis., 41, 57
Rubin, R. H. 1989, ApJS, 69, 897
Sabbadin, F., Minello, S., & Bianchini, A. 1977, A&A, 60, 147
Sandstrom, K. M., Bolatto, A. D., Stanimirović, S., van Loon, J. T., & Smith, J. D. T. 2009, ApJ, 696, 2138
Spezzi, L., Merin, B., Oliveira, I., van Dishoeck, E. F., & Brown, J. M. 2010, A&A, 513, A38
Stanghellini, L., García-Lario, P., García-Hernández, D. A., et al. 2007, ApJ, 671, 1669
Stupar, M., Parker, Q. A., Filipović, M. D., et al. 2007, MNRAS, 381, 377
Werner, M. W., Gallagher, D. B., & Irace, W. R. 2004, Adv. Space Res., 34, 600

---

[3] The data are publicly available and can be accessed through the data archives at ESO and the *Spitzer* Science Center:
http://archive.eso.org/eso_archive_main.html
http://ssc.spitzer.caltech.edu/spitzerdataarchives/